Stem Cell Research (2009) 2, 198–210

available at www.sciencedirect.com

www.elsevier.com/locate/scr

REGULAR ARTICLE

Teratoma formation by human embryonic stem cells: Evaluation of essential parameters for future safety studies

Hannes Hentze [a,*,1], Poh Loong Soong [a,2], Siew Tein Wang [a,3], Blaine W. Phillips [a,4], Thomas C. Putti [b], N. Ray Dunn [a,3]

[a] *ES Cell International Pte Ltd, 60 Biopolis Street, No. 01-03 Genome, Singapore, 138672 Singapore*
[b] *Department of Pathology, National University Health System, 5 Lower Kent Ridge Road, 119074 Singapore*

Received 5 December 2008; received in revised form 23 January 2009; accepted 4 February 2009

Abstract Transplantation of human embryonic stem cells (hESC) into immune-deficient mice leads to the formation of differentiated tumors comprising all three germ layers, resembling spontaneous human teratomas. Teratoma assays are considered the gold standard for demonstrating differentiation potential of pluripotent hESC and hold promise as a standard for assessing safety among hESC-derived cell populations intended for therapeutic applications. We tested the potency of teratoma formation in seven anatomical transplantation locations (kidney capsule, muscle, subcutaneous space, peritoneal cavity, testis, liver, epididymal fat pad) in SCID mice with and without addition of Matrigel, and found that intramuscular teratoma formation was the most experimentally convenient, reproducible, and quantifiable. In the same experimental setting, we compared undifferentiated hESC and differentiated populations enriched for either beating cardiomyocytes or definitive endoderm derivatives (insulin-secreting beta cells), and showed that all cell preparations rapidly formed teratomas with varying percentages of mesoderm, ectoderm, and endoderm. In limiting dilution experiments, we found that as little as two hESC colonies spiked into feeder fibroblasts produced a teratoma, while a more rigorous single-cell titration achieved a detection limit of 1/4000. In summary, we established core parameters essential for facilitating safety profiling of hESC-derived products for future therapeutic applications.

Introduction

Human embryonic stem cells (hESC) are derived from the inner cell mass of blastocyst-stage preimplantation embryos. hESC are characterized by their cardinal properties of self-renewal and pluripotency, i.e., the ability to differentiate into derivatives of the three embryonic germ layers. Since hESC were first isolated in 1994 (Bongso et al., 1994) and later shown to propagate as individual lines *in vitro* (Thomson et al., 1998), they have attracted enormous attention due to their potential use as raw material for the production of therapeutically useful cell types such as

Abbreviations: hESC, human embryonic stem cells; mESC, mouse embryonic stem cells; PBS, phosphate-buffered saline.

* Corresponding author. Fax: +65 68725005.
E-mail address: hannes_hentze@sbio.com (H. Hentze).
[1] Present address: S*BIO Pte Ltd, 1 Science Park Road, No. 05-09 The Capricorn, Singapore Science Park II, 117528 Singapore.
[2] Present address: Zentrum Pharmakologie und Toxikologie der Universität Göttingen, Robert-Koch-Strasse 40, 37075 Göttingen, Germany.
[3] Present address: Institute of Medical Biology, 8A Biomedical Grove, No. 06-06 Immunos, 138648 Singapore.
[4] Present address: Lilly Singapore Center for Drug Discovery Pte Ltd, 8A Biomedical Grove, No. 02-05 Immunos, 138664 Singapore.

1873-5061/$ – see front matter © 2009 Elsevier B.V. All rights reserved.
doi:10.1016/j.scr.2009.02.002

pancreatic β cells, cardiomyocytes, and motor neurons (Hentze et al., 2007; Keller, 2005; Vogel, 2005). This prospect has led to the development of numerous *in vitro* directed differentiation protocols. To date, however, most preparations of differentiated hESC are merely enriched for the cell type of interest, and the presence of unknown, confounding, and possible tumor-promoting cell types raises broad alarm about not only the future clinical efficacy of this material but also its safety.

hESC like their mouse counterpart cells form benign tumors in immunodeficient mice (Damjanov and Andrews, 2007; Solter, 2006). These tumors are reminiscent of spontaneous human teratomas that arise most commonly in the gonads and comprise to varying degrees endodermal, mesodermal, and ectodermal derivatives (Gertow et al., 2007). Thus, this *in vivo* assay serves as a robust and relatively simple way to demonstrate pluripotency. Furthermore, given the obvious ethical challenges concerning the generation of chimeric embryos by injecting hESC into supernumerary human blastocysts (Leist et al., 2008) and the poor contribution of hESC when transplanted into mouse host blastocysts, teratoma formation essentially serves as the only available measure for confirming pluripotency *in vivo* (Adewumi et al., 2007; Brivanlou et al., 2003; Gertow et al., 2007). For example, amniotic stem cell lines were recently shown to exhibit incomplete pluripotency, while human-induced pluripotent stem (iPS) cells readily formed bona fide teratomas in SCID mice (De Coppi et al., 2007; Takahashi et al., 2007; Yu et al., 2007).

A series of recent studies shows that teratoma formation is strongly dependent on the site of engraftment. Teratomas have been produced by hESC transplantation into the testis (Gertow et al., 2004; Przyborski, 2005; Stojkovic et al., 2005), kidney capsule (Blum and Benvenisty, 2007), liver (Cooke et al., 2006), hind leg muscle (Amit et al., 2003; Choo et al., 2004; Plaia et al., 2006; Tzukerman et al., 2006) and and into the subcutaneous space (Cooke et al., 2006; Prokhorova et al., 2008). Two recent studies systematically compared teratoma formation in diverse locations (Cooke et al., 2006; Prokhorova et al., 2008); they both concluded that subcutaneous implantation is most permissive. However, neither of these studies comprehensively examined teratoma growth over time or attempted to define a minimum number of cells required to seed a teratoma. In contrast, Lawrenz et al. (2004) performed rigorous titration studies with an emphasis on teratoma growth kinetics and detection limits using mouse embryonic stem cells (mESC). Defined numbers of single-cell mESC (the J1 line) were mixed with a population of non-neoplastic MRC-5 fibroblasts before injection into immunocompromised mice (Lawrenz et al., 2004). The detection limit of this assay was determined to be 20 individual mESC spiked into a 2×10^6 cell inoculum in 100% of attempts, i.e., 1×10^{-5} or 0.001%. Similarly, establishing the sensitivity of the teratoma assay on a per cell basis and standardizing how teratoma formation is measured across laboratories will allow the tumor-forming potential of cell populations intended for transplantation to be carefully quantified and to address systematically the mounting regulatory requirements promulgated by the US Food and Drug Administration, FDA (Halme and Kessler, 2006).

In our previous studies, we found that hESC differentiated for extended periods of time were still able to form teratomas (Phillips et al., 2007; Xu et al., 2008). In contrast, several other reports characterizing differentiated hESC (Kroon et al., 2008; Laflamme et al., 2005; Reubinoff et al., 2001; Tomescot et al., 2007; Zhang et al., 2001) or mESC (Guo et al., 2006; Kumashiro et al., 2005) populations observed infrequent to no teratoma formation in various animal models. Several of these prior studies suffer from the entire absence of positive controls, insufficient *in vivo* time scales, or lack of histological and immunocytochemical characterization of the recovered hESC-derived material. Having future hESC safety studies in mind, we initiated a series of experiments guided by the mESC study of Lawrenz et al. (2004). We used a number of hESC lines in SCID mice and found that intramuscular injection is the most robust location for teratoma formation and also easiest to grade. We were further able to correlate hESC numbers and teratoma growth kinetics when using defined numbers of hESC colonies or trypsin-adapted hESC spiked into supportive feeder cells.

Results

Site-dependent formation and grading of hESC teratomas in SCID mice

In a limited series of initial experiments, we explored a variety of transplantation sites for their susceptibility to form hESC-derived teratomas with the aim of identifying one that is easy to inject and readily allows teratoma formation. Additionally, the requirement of Matrigel for teratoma formation was assessed (Fig. 1A). We were interested in evaluating whether teratomas occur in all locations, and whether each site promotes excessive formation of cysts. We found that *all* teratomas that grew within 8 weeks after hESC injection in the kidney capsule, body cavity (intraperitoneal/ip), testis, epididymal fat pad, and liver parenchyma contained pronounced liquid-filled cysts, which hampered histological analysis. Notably, injection of hESC subcutaneously gave rise to palpable teratomas when Matrigel was coinjected (3/3 animals) but not in the absence of Matrigel (3/3 animals). These tumors grew slowly, were cyst free, dense, and hard to process for histology. In our hands, hESC teratomas formed well without Matrigel and in the absence of any cyst formation when injected intramuscularly (im, 3/3 animals). Although the animal numbers of this study were low, we confirmed this positive result using numerous hESC lines in subsequent experiments. Intramuscular teratomas were robustly generated with hES2 and hES4 (not shown), and with the cGMP (current good manufacturing practice)-compliant lines ESI-014, ESI-017, ESI-035, ESI-049, ESI-051, and ESI-053 (Crook et al., 2007). Fig. 1B illustrates the typical histology of a mature well-differentiated teratoma with all three germ layers (endoderm, mesoderm, and ectoderm).

We next characterized the intramuscular teratomas further by immunhistochemistry with typical differentiation markers: anti-desmin staining (Fig. 2A) revealed smooth muscle layers (mesoderm); anti-GFAP staining (Fig. 2B) detected the dispersed presence of glia-like structures

A

	Matrigel Required	Teratoma Formation in <8 Weeks	Formation of Cysts	N
Kidney Capsule	-	+	+	3
Intramuscular (*i.m.*)	-	+	-	3
Subcutaneous (*s.c.*)	+	-	-	6
Intraperitoneal (*i.p.*)	-	+	+	6
Testis	-	+	+	3
Liver	-	+	+	3
Epididymal Fat Pad	-	+	+	6

B

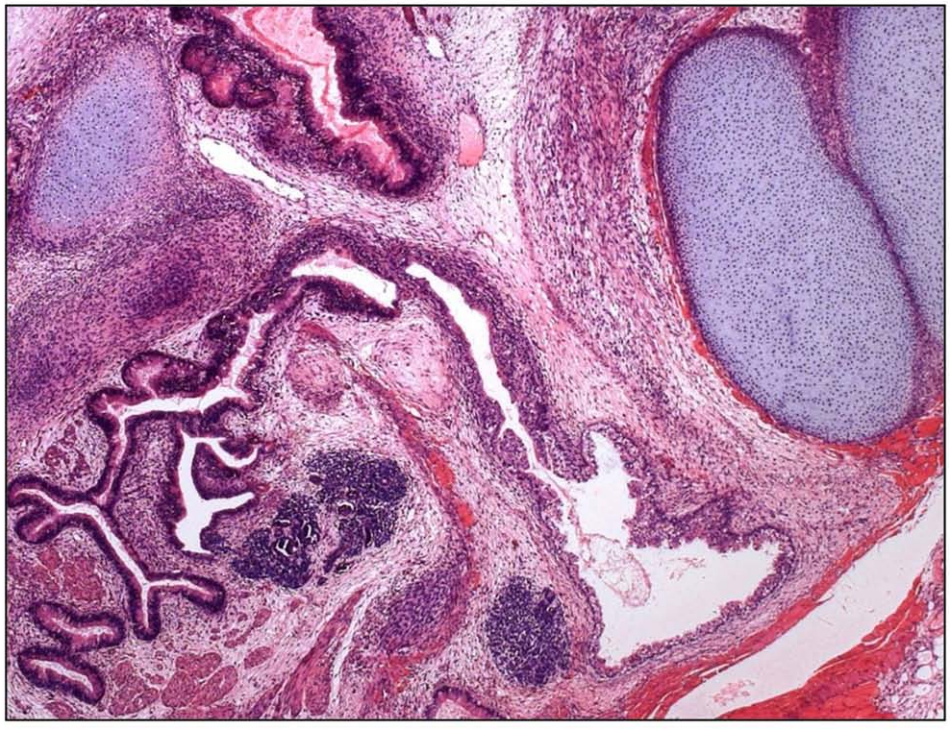

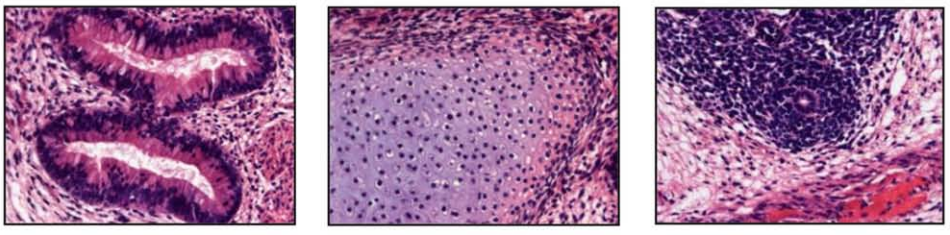

End Mes Ect

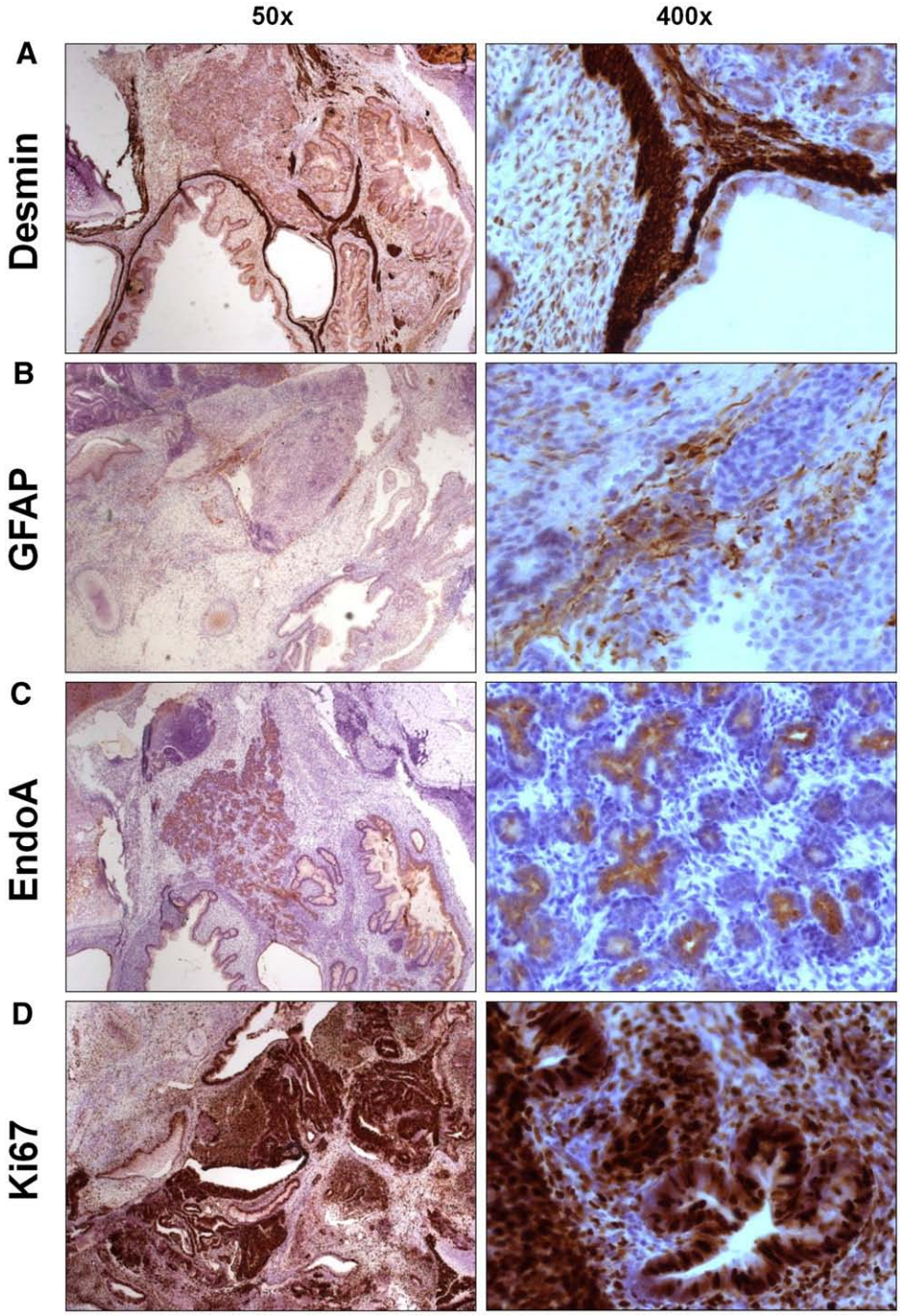

Figure 2 Presence of all three primary germ-layer derivatives in a prototypical intramuscular teratoma. Sections from a single 12-week intramuscular teratoma were stained with assorted antibodies: (A) anti-desmin (mesoderm/muscle); (B) anti-GFAP (ectoderm/neural epithelium); (C) anti-endoA (keratinized endodermal epithelium); and (D) anti-Ki67 (proliferating cells). Magnifications as indicated.

(ectoderm); and anti-endoA keratin staining showed typical glandular endodermal structures (Fig. 2C). We also performed anti-Ki67 staining which identifies proliferating cells. We observed areas of very intense proliferation, where almost every present cell was positive, and others with very low levels of proliferation (Fig. 2D).

Figure 1 Teratoma formation after injection of hESC in different anatomical locations. (A) Approximately 10^6 hESC in clumps were injected in seven different engraftment locations into individual SCID mice. All mice were sacrificed after 8 weeks, and teratoma growth was assessed. The requirement for Matrigel for teratoma growth, the development of detectable teratomas, and the formation of obvious cysts within the teratoma are summarized ($n = 3$ or 6 mice/group as indicated). (B) Typical histology of a well-differentiated intramuscular teratoma harvested after 12 weeks. Upper panel, low magnification (5×). Lower panels, End (endodermal), Ect (ectodermal), and Mes (mesodermal) structures at high magnification (40×).

Because teratomas are readily visible in the intramuscular location and because we intended to quantify our studies, we developed a generic and fast scoring method that allowed us to screen large numbers of animals without using a caliper (Fig. 3A): no teratoma is assigned grade 0; when a teratoma becomes just detectable the animal is scored with "1"; when the teratoma is clearly visible we score the animal with "2"; and only when the teratoma is large and impedes locomotion we grade it "3", which coincides with the time of harvest. Fig. 3B confirms the robustness of this method by comparing it to caliper measurements; note that the diameters of hind legs with grade 1 teratomas are on average significantly different compared to controls (6.32 mm on a normal hind leg of a naïve mouse compared to 10.55 mm at grade 1). Other figures throughout this paper show data derived by this simple scoring method.

Teratoma formation by differentiated cell populations

To attempt to quantify differences in tumor-forming capacity in hESC populations, we next applied our intramuscular scoring to characterize differentiated hESC populations. Fig. 4A shows the growth kinetics of undifferentiated hESC in comparison to hESC that were differentiated according to a 12-day cardiomyocyte protocol (Graichen et al., 2007) or a lengthy 42-day protocol that induces beta-like cells from hESC (Phillips et al., 2007). We found that the growth kinetics of teratoma formation among the three different cell populations were similar, showing that high numbers of pluripotent cells were still present in all three cell preparations. This result clearly illustrates the safety concerns associated with purportedly "differentiated" hESC-derived material intended for human transplantation.

Histological characterization of teratoma specimens by a certified pathologist revealed that the germ-layer distribution was slightly altered when differentiated cells were used. Teratomas derived from undifferentiated hESC cultures have a significant bias toward mesoderm (67%), with little endodermal (20%) and even less ectodermal (13%) components (Fig. 4B). We found throughout our studies that this germ-layer distribution for hES3 was similar when numerous alternative hESC lines were tested as undifferentiated cell populations in the same im model. We present an overview of representative data of germ-layer distributions of six cGMP-compliant hESC lines in Suppl. Fig. 1A, in which average percentages (68% mesoderm, 19% endoderm, and 13% ectoderm) approach the hES3 data (Fig. 4B). Notably, cardiomyocyte-like cell populations derived from hESC gave rise to teratomas with more than double the endodermal component at the expense of mesoderm/ectoderm (Fig. 4B, Suppl. Fig. 2A), which is in line with the upregulation of endodermal markers such as *Sox17* observed in the latter differentiation protocol (Graichen et al., 2007). This shift was less pronounced when beta cell-like hESC cultures were used. It is noteworthy that in contrast to the germ-layer distribution observed in the teratomas shown in Figs. 1, 2, and 6 and in Suppl. Fig. 2B, most spontaneous mature

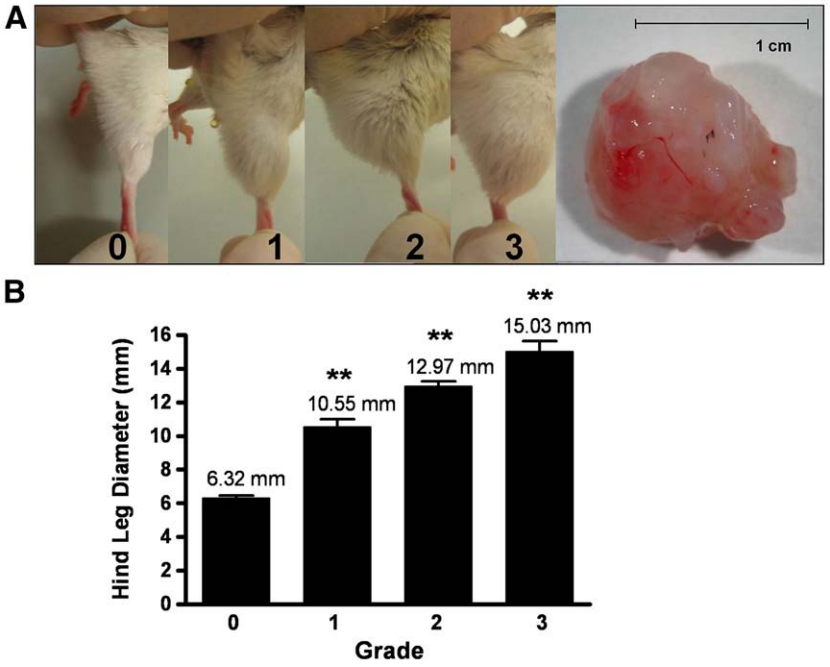

Figure 3 Development of a simple grading system for visible intramuscular teratomas. (A) Approximately 10^6 hESC in clumps were injected into the hind leg of individual SCID mice. A simple grading scale for monitoring teratoma development is shown: 0 = no teratoma; 1 = teratoma just visible; 2 = teratoma clearly visible; and 3 = large teratoma, locomotion impeded. Teratomas are routinely harvested when grade 3 is achieved. The right panel shows the gross morphology of a grade 3 teratoma, with a typical weight ≥ 1 g. (B) The maximum upper hind leg diameters were measured using a manual caliper ($n = 10$ mice/group). The average diameters (±SD) correlate well with the grade assigned by simple visual inspection. Note that even the hind leg diameter for grade 1 is significantly different from the hind leg diameter of naïve animals (one-way ANOVA/Bonferroni; ** indicates a P value < 0.01).

A

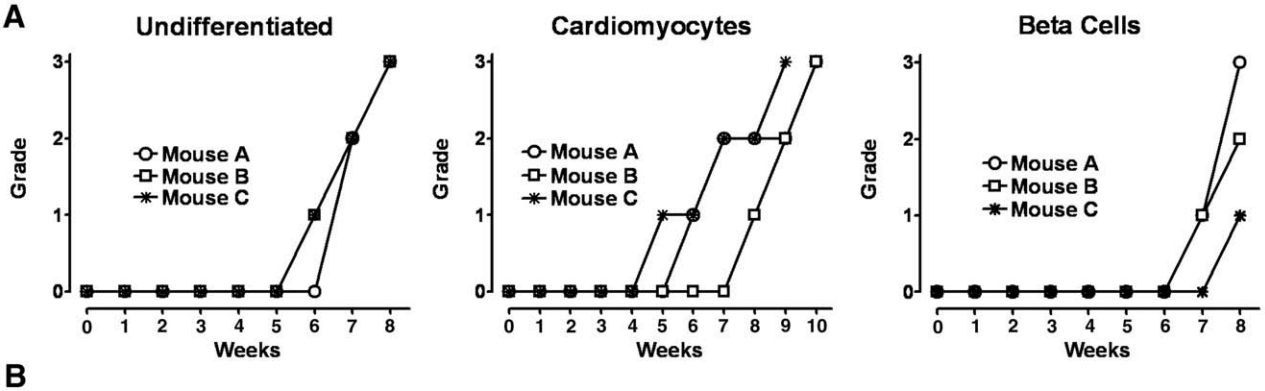

B

	Percentage Germ Layer			
	Endoderm	Ectoderm	Mesoderm	n
Undifferentiated (*i.m.*)	20%	13%	67%	8
Cardiomyoctes (*i.m.*)	47%	8%	45%	3
Beta Cells (*i.m.*)	25%	15%	60%	1
Beta Cells (Kidney)	27%	21%	52%	5

Figure 4 Teratoma formation initiated with either undifferentiated or differentiated hESC populations. (A) Undifferentiated hESC (left), hESC subjected to cardiomyocyte differentiation (middle), or hESC differentiated according to a multistep protocol favoring definitive endoderm/beta cell generation (right) were injected as cell clumps intramuscularly (approximately 10^6 cells/mouse). Teratoma formation was visually assessed according to the method described in Fig. 3. All injected cell populations formed detectable tumors within 8 weeks. (B) Histopathological distribution of primary germ-layer derivatives in teratomas of assorted hESC origins (for teratoma histology pictures, see Suppl. Fig. 2A). The first three cell preparations were injected im, except that beta cells were injected im and into the kidney capsule. The *n* numbers given refer to germ-layer assessments for independent experiments. Average percentage of tissue prevalence ± SD is shown.

teratomas occurring in humans are histologically much more biased toward ectoderm (>50%, Suppl. Fig. 1B), and they are mostly benign teratomas categorized as type I (Blum and Benvenisty, 2008). These spontaneous human teratomas are often cystic, and presumably derived from ectodermal differentiation of pluripotent cells close to ES cells.

Titration of colonies of undifferentiated hESC in the im SCID model

We next aimed to increase the sensitivity of the im SCID model, with the ultimate goal of possibly quantifying the minimal number of undifferentiated hESC capable of seeding a teratoma. hESC in clumps or colonies were mixed with known numbers of nontumorigenic CCD919 human foreskin fibroblasts that serve as an inert substrate. We also reasoned that using a fibroblast line used in hESC culture may increase the sensitivity of the teratoma model, compared to other non-neoplastic cells similar to the study of Lawrenz et al. (2004). hESC clumps expectedly gave rise to teratomas in 3/3 mice within 6 weeks, whereas only 2/3 mice inoculated im with 10 hESC colonies (approximately 30 000 hESC/colony) developed teratomas within 11 weeks (Fig. 5A). Spiking 10 hESC colonies into CCD919 fibroblasts accelerated teratoma formation significantly, and increased the take rate (3/3 teratomas in 8 weeks). CCD919 never formed a tumor mass (Fig. 5A), even beyond 20 weeks (not shown). We next addressed whether increasing numbers of hESC colonies spiked into CCD919 fibroblasts would decrease the time required for teratoma formation. We mixed 2, 5, 10, and 20 colonies with 10^6 CCD919 fibroblasts (Fig. 5B). Indeed, 20 colonies/animal rapidly formed teratomas in 3/3 animals that were detectable after only 5 weeks, reached grade 3 at week 8, and at this point were fully mature displaying a haphazard arrangement of tissues representative of all 3 germ layers (Suppl. Fig. 2B). Consistently, 5 and 10 colonies formed teratomas more slowly, and 2 colonies were slowest, requiring a full 12 weeks to yield a detectable tumor in 3/3 animals. When the colony number was plotted against the time required to detect teratomas, a strong linear correlation was observed ($r^2 = 0.95$, Fig. 5C). In summary, it is possible to approximately correlate hESC numbers with the time required for teratoma growth in a sensitive system such as the described CCD919 spiking/SCID mouse model.

Titration of single-cell suspension in the im SCID model

Finally, we performed a number of experiments where we mixed single-cell hESC dispersed by trypsin digestion with 10^6 CCD919 fibroblasts in order to define the minimal hESC number required to seed teratoma formation (Fig. 6). In the experiment shown in Fig. 5A, the largest hESC bolus (2×10^6 cells) gave rise to a detectable tumor within only 3 weeks and reached grade 3 at week 5 (Fig. 6A), whereas the lowest number of hESC (245 cells) required 12 weeks until grade 3 of

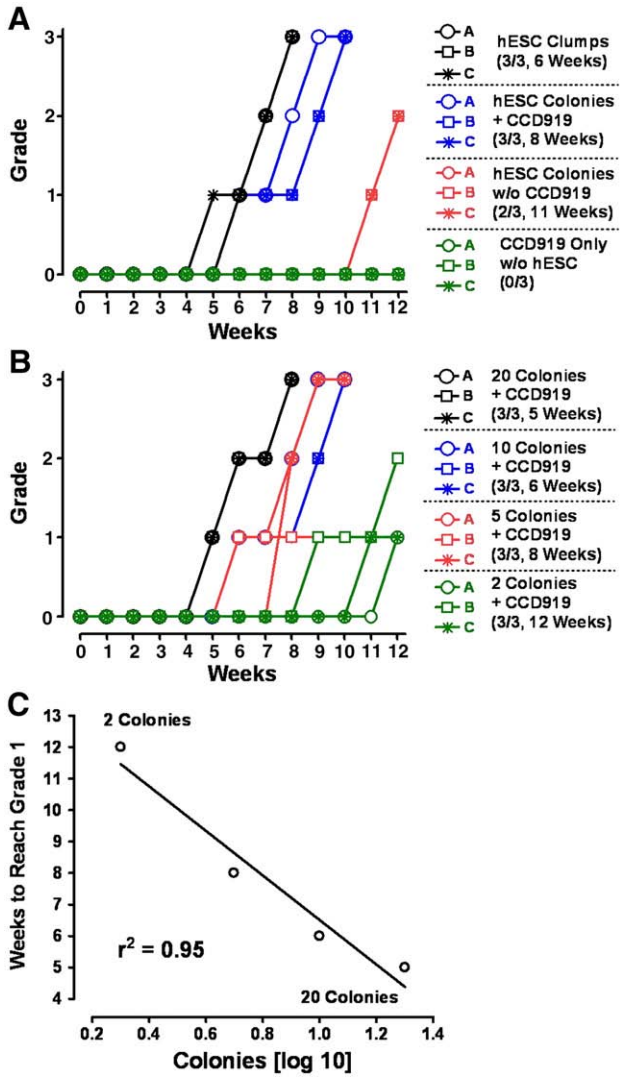

Figure 5 Teratoma formation on injection of limiting numbers of hESC colonies. (A) Approximately 10^6 hESC in clumps, intact hESC colonies alone or in combination with 10^6 mitomycin C-treated CCD919 feeder cells, or feeder cells alone were injected into the hind leg of SCID mice as indicated. Teratoma formation was visually assessed according to the method described in Fig. 3 (3 mice/group for all conditions). (B) Decreasing numbers of hESC colonies were mixed with 10^6 mitomycin C-treated CCD919 cells and injected intramuscularly (3 SCID mice/group). (C) Correlation of hESC colony number (log 10) with the time required to achieve grade 1 (in weeks). For histology, see Suppl. Fig. 2B.

a teratoma was achieved. Again, we observed a linear highly correlative relationship between cell number and time required to reach grade 1 as shown in Fig. 6B. Notably, the harvested teratoma at week 5 generated from 2×10^6 hESC displayed a stromal immature tumor histology (Fig. 6C), classifying this lesion as an immature teratoma. Tumors with a similar histological appearance in human patients are considered malignant (teratocarcinomas) and are routinely treated based on their grade and stage. In contrast, a teratoma harvested at week 8 derived from a bolus of 1950 hESC showed a fully mature phenotype with all three germ layers present (Fig. 6C).

Repeating this study format with various cultures of hES3 (as used throughout Figs. 1–5), we noted that varying success of teratoma formation did not correlate with an abnormal karyotype or with passage number, but rather with the cell subline adaptation to trypsin digest. We more systematically addressed this difference with an independent hESC line in Figs. 6D and E. Collagenase-passaged ESI-017 hESC did not generate teratomas when single-cell digested with trypsin and spiked into CCD919 cells as described above, whereas trypsin-adapted (>5 passages) ESI-017 hESC (Ellerstrom et al., 2007; Hasegawa et al., 2006; Phillips et al., 2008a, 2008b) readily gave rise to teratomas, at least when higher cell numbers >1000 cells were used. Importantly, the single-cell-adapted ESI-017 line used in our experiments was karyotyped and used at passages below 30. This line maintained a normal, diploid karyotype at least up to passage 39 (cf. Fig. 2B in Phillips et al., 2008b). We conclude that it is possible to generate teratomas from low numbers of single-cell hESC, but the success of this approach depends on the specific hESC line and its trypsin adaptation.

Discussion

A number of recent publications addressed various aspects of teratoma formation from hESC such as terminology, clonality of tumors, and transplantation sites (Blum and Benvenisty, 2007, 2008; Damjanov and Andrews, 2007; Lensch and Ince, 2007; Prokhorova et al., 2008), but none of these confronted experimentally the important quantification and safety concerns regarding future cell therapy products derived from hESC (reviewed in Halme and Kessler, 2006; Hentze et al., 2007). In our study, we sought to establish several critical parameters for future hESC safety studies such as the robustness of teratoma formation, quantification, time scale, and the minimal cell numbers required to form a teratoma. We found that hESC cell injection into the hind leg of SCID mice reproducibly generated fully differentiated teratomas that can be easily graded and followed over time, even when using 1/4000 (or 0.025%) of undifferentiated hESC spiked into nontumorigenic feeder fibroblast cells that support hESC growth *in vitro*. Figs. 5 and 6 suggest that the high reproducibility and sensitivity of our SCID model are directly attributed to mixing hESC with feeder cells. Further studies using single-cell-adapted hESC cultures will determine whether the absolute detection limit can be increased further, a goal which is predicated on the development of experimental methods that produce viable single-cell suspensions of hESC (Ellerstrom et al., 2007; Hasegawa et al., 2006; Phillips et al., 2008a, 2008b).

During a meeting in April 2008 organized by the US FDA, Geron, a biotech company based in Menlo Park, California, showed that undifferentiated hESC when mixed with non-tumorigenic, hESC-derived oligodendroglial progenitor cells and injected into the spinal cord of immunodeficient mice developed teratomas within 12 months only when 10% or more of hESC were present (FDA, 2008b). For comparison, the FDA/CBER 2006 guideline recommends testing 10^8 vector-producing cells for the presence of any replication-competent retrovirus, assuming the assay would be sensitive enough to pick up a single infected cell, a number many magnitudes greater than the current techniques available for

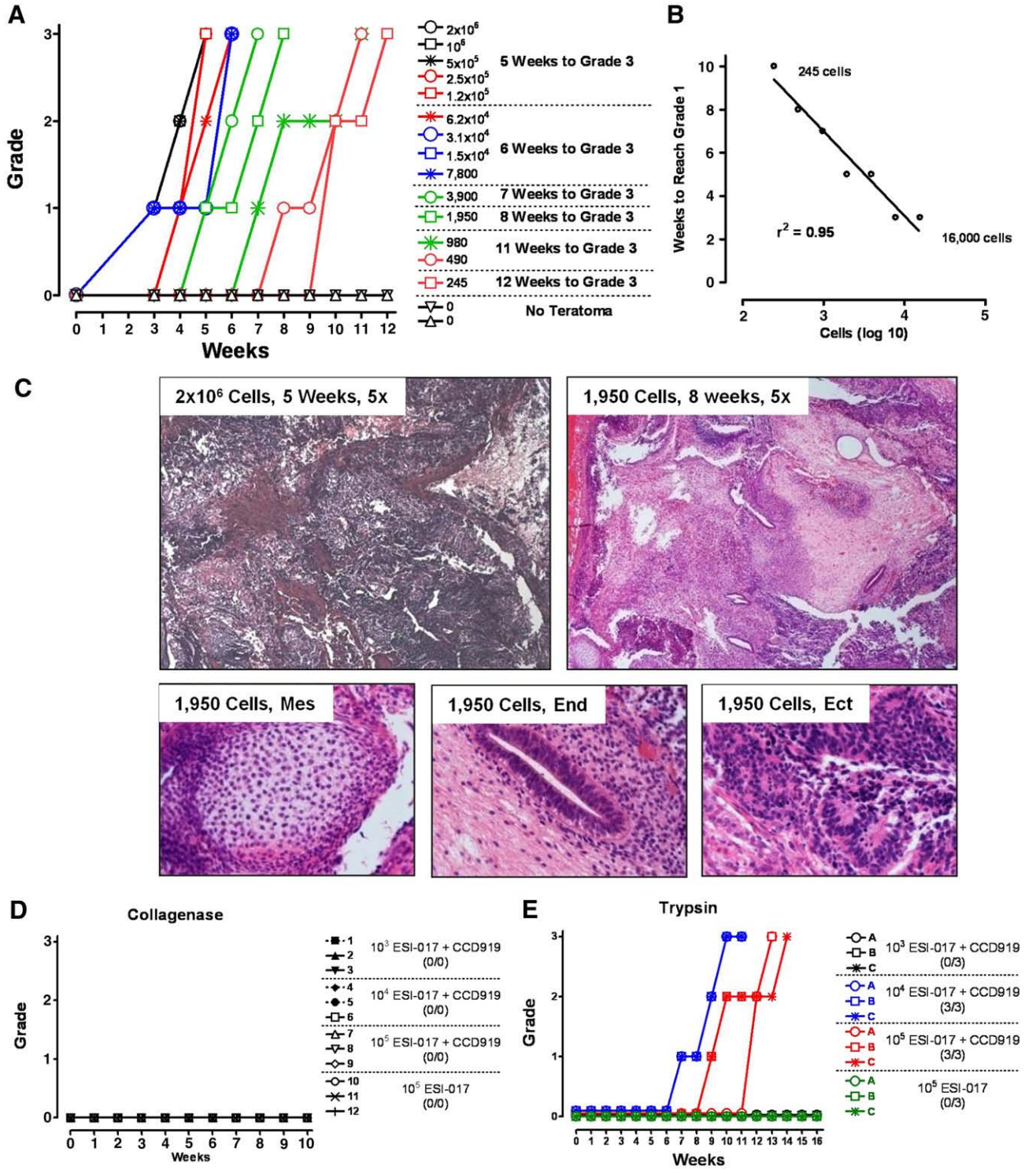

Figure 6 Teratomas formed by limiting dilutions of hESC spiked into human feeder cells. (A) Serial dilutions of trypsinized single-cell hESC were mixed with 10^6 mitomycin C-treated CCD919 human feeder cells before injection intramuscularly into SCID mice. Feeder only injections served as negative controls. Mice were visually monitored for as many as 12 weeks, and were euthanized whenever a grade 3 teratoma was observed. (B) Values in A were converted and replotted as a correlation between log hESC number (*x*-axis) and time in weeks until a grade 1 teratoma was detected. (C) Comparison between teratomas generated from 2×10^6 and 1950 hESCs. Detailed histological analysis of the 1950 hESC-derived teratoma reveals hypernucelated neuroectodermal structures; glandular endoderm; cartilage surrounded by ossified structures (mesodermal origin). (D) The hESC line ESI-017 (grown on human feeders) was passaged by Collagenase digest for more than 5 passages, trypsinized into single cells, spiked into CCD919 fibroblasts, and then injected as shown in A; no teratomas emerged. (E) Similarly, ESI-017 (grown on human feeders) was passaged by trypsin digest for more than 5 passages, trypsinized into single cells, spiked into CCD919 fibroblasts, and injected as shown in A. Here, teratomas emerged when 10^4 or 10^5 cells per animal, but not when 10^3 cells, were used. Without spiking into CCD919 fibroblasts, no teratomas were detected as well.

quantifying residual hESC numbers (FDA, 2006). The hESC detection limit established in our current study would be sufficient to detect the difference between hESC contamination of 1/1000 and 1/10 000; one would theoretically require 100 mice to test a 10^8 hESC bolus. The question nevertheless remains which safety margins will eventually be set by the FDA for all future hESC applications (FDA, 2008a; Hentze et al., 2007).

One critical variable for hESC safety studies is the immune status of the host mouse strain, as it is evident that the teratoma assay becomes increasingly more sensitive the greater the immune deficiency. A study by Drukker et al. established that T cells play a crucial role in the xenorejection of implanted hESCs by comparing undifferentiated hESCs in immunocompetent versus immunodeficient mice (Drukker et al., 2006). Immunocompetent mice did not develop teratomas within a month, whereas immunodeficient mice differed in their ability to reject hESCs (e.g., NOD/SCID mice developed tumors). Another study compared the susceptibility of NOD/SCID (no B, T cells) versus SCID/Beige mice (no B, T, NK cells) toward teratoma formation after intramuscular implantation of hESCs. Tumors grew significantly faster in the SCID/Beige mice, suggesting that NK cells play a major role in xenorejection of implanted hESCs (Tian et al., 2006). This result was confirmed in a recent study performed with mESC in a xenogenic rat model (Dressel et al., 2008). In agreement with the notion above, we observed that in our SCID mice experiments, suboptimal cell viability indeed can lead to failure of hESC cell engraftment. It may therefore be possible to greatly increase the sensitivity of this teratoma model by several magnitudes with fully immunocompromised mice (e.g., NOD/SCID/IL2Rγ^{null}) and much longer observation periods. In addition, it is noteworthy in this context that in the cancer stem cell field, at least two recent studies managed to increase the detection limit of rare cancer stem cells in a primary tumor—typically cited at around $1/10^6$. By using NOD/SCID/IL2Rγ^{null} or nonirradiated congenic mice, extending the observation period to many months and applying Matrigel, the frequency of tumor-initiating cancer stem cells was found to be in the area of 4–10% rather than 0.001% (Kelly et al., 2007; Quintana et al., 2008). Another important consideration is a potential drawback due to differences in tumor growth kinetics and immune status when using immunodeficient mice as a xenogenic system for safety studies. As discussed in detail elsewhere (Hentze et al., 2007), the sensitivity of such safety studies may be greatly enhanced by using better immunodeficient mouse strains or by spiking hESC into suitable cellular substrates (Fig. 6). These assays may still be magnitudes less sensitive compared to the transplantation into a patient for three reasons: (i) most importantly, the time scales of such *in vivo* experiments greatly differ, and even if we were to extend the safety models to 6 or even 12 months, we expect a future cell therapy product to persist in the patient for years which poses a problem as little is known about the potential safety issues with low numbers of long-time surviving undifferentiated hESC; (ii) the effects of interspecies transplantation on the efficacy of engraftment and tumorigenicity are largely unknown; and (iii) the effective difference between immunosuppression versus immunodeficiency on the outcome on such experiments may be another crucial factor to be considered. A recent study by Shibata et al. illustrates all the above factors (Shibata et al., 2006). Unselected hematopoietic precursors differentiated from Cynomolgus monkey embryonic stem cells did not form tumors when transplanted into immunodeficient SCID mice (xenogenic, immunodeficient) or in fetal sheep liver (xenogenic, immunoprivileged), but they did form lethal tumors within 2–3 months when transplanted back into Cynomolgus monkeys (autologous, no immune suppression/deficiency), demonstrating that autologous hESC transplantation is much more conducive to tumor formation when compared to any other setting.

It is generally believed that extended *in vitro* differentiation results in decreased teratoma formation, as exemplified in an earlier study using hESC differentiated into neuronal cells and transplanted into rat brains (Brederlau et al., 2006). Remarkably, a recent paper by Kroon et al. showed that hESC-derived preparations of predominantly definitive endoderm/pancreatic progenitors rarely formed teratomas (1/46 or 2.2%) when transplanted into the epididymal fat pad (Kroon et al., 2008). In contrast, our own studies (cf. Fig. 4A) and comparable studies using endodermal and cardiomyocyte differentiation protocols of ESC (Cai et al., 2007; Fujikawa et al., 2005; Graichen et al., 2007; Phillips et al., 2007) showed that ESC differentiated even over extended periods of time are still able to form teratomas. Again, at present there is no formal FDA guideline on how the contamination of a given clinic-ready cell population by hESC should be measured in a "gold standard" tumor assay.

Can teratoma formation be prevented experimentally prior to transplantation of clinical material of hESC origin? One potential method is to eliminate rogue undifferentiated cells by selectively removing them based on their well-defined cell-surface marker profile (e.g., SSEA-4^+, Tra1-60^+, and Tra1-81^+) using a combination of antibodies and sorting by FACS or MACS (reviewed in FDA, 2008a; Hentze et al., 2007). An alternative antibody-based approach was recently described that employed a cytotoxic monoclonal antibody (mAb 84) that recognizes the cell-surface molecule Podocalyxin-like Protein-1 that is specifically expressed on undifferentiated, but not differentiated, hESC (Choo et al., 2008). In our own laboratory using the described im SCID mouse model, we found that teratoma formation was eliminated in SCID mice when hESC or NCCIT embryonal carcinoma cells were pretreated with mAb 84 prior to hind limb injection. Despite the promise of these techniques, several challenges exist, including the development and expense of cGMP-compliant antibodies, the preparation of differentiated hESC that are viable as single cells and, importantly, remain efficacious after transplantation, and the length of time of the selection technique itself. A genetic-based selection technique that is very effective at eliminating teratoma formation in the im SCID mouse model has also been described (Xu et al., 2008): Xu et al. from ES Cell International engineered hES-3 to express the neomycin-resistance gene under the control of the cardiomyocyte-specific α-myosin heavy chain (α-MHC) promoter. Differentiation and G418 selection produced nearly 100% pure cultures of cardiomyocytes. Notably, intramuscular transplantation of approximately 1×10^6 of these cells yielded no teratomas. This encouraging result suggests that highly purified progenitors or terminally differentiated cell types derived from hESC will mitigate the safety concerns

surrounding heterogeneous cell preparations and the tumor-promoting cells they conceal.

There are numerous disagreements among the teratoma studies in the current literature, which can be attributed to different experimental settings, minute procedural details, or interpretation of results. In our experience, even minor variations in cell harvest procedures (centrifugation, pipetting), in timing from cell harvest to inoculation (<1 h), and most importantly in the injection procedure itself (which requires two trained operators, one to restrain the animal and one to inject the cells) can hamper reproducibility. For this reason, we rigorously used SOPs and detailed record sheets for these experiments. For instance, a recent report by Prokohora et al. found that the muscle is inferior to the subcutaneous space for hESC injection as only 1 of 8 mice developed a teratoma (Prokhorova et al., 2008). However, the methods for injection, the hESC lines, and hESC culture methods as well as the mouse strains used all differed from our study. Furthermore, the animal numbers in the above study as well as in our pilot study comparing different anatomical locations (Fig. 1) are quite limited due to the resource-intensive nature of such comparative *in vivo* studies. Lastly, submicroscopic changes such as SNP profile changes that, for instance, influence the replating efficiency of hESC lines (Hasegawa et al., 2006) may also contribute to differences in teratoma formation, an issue that would warrant additional comparative teratoma studies. As another example, the insulin-producing hESC-derived grafts recovered after 56 days in a study by Eshpeter et al. display bona fide teratoma histology (Eshpeter et al. 2008; Kroon et al., 2008), similar to outgrowths described in our own previous work (Phillips et al., 2007). Although the authors provide evidence of moderate clinical efficacy, the important question of tumorigenicity and safety cannot be overlooked. In conclusion, a gold standard for testing hESC-derived cell therapy products in an *in vivo* model is highly desirable for comparing the potential safety issues arising from these heterogeneous preparations.

Materials and methods

hESC culture

For most experiments, hES3 (Reubinoff et al., 2000) or its derivate GFP-hES3 (Costa et al., 2005) were used; additional hESC lines hES2, hES4, ESI-014, ESI-017, ESI-035, ESI-049, ESI-051, and ESI-053 were employed where indicated. hESC were grown on γ-irradiated human foreskin fibroblasts (CCD919, ATCC) (Crook et al., 2007), routinely plated at a density of 3×10^5 cells/cm^2. Prior to use, feeder plates were conditioned overnight in hESC medium containing KO-DMEM, 1% nonessential amino acids, 1×penicillin/streptomycin, 2 mM L-glutamine, and 20% KOSR (all reagents from Invitrogen) and supplemented with 50 μg/ml bFGF (Strathman). hESC passaging or harvesting was performed using Collagenase NB6 (Serva, 1.25 mg/ml for 4 min). Treated plates were rinsed with PBS and replenished with hESC medium. The entire surface area of the plate was then streaked with a 2 ml disposable plastic pipette at approximately 2-mm intervals. The cells were harvested with a cell scraper and transferred to new feeder plates. The cells were split every 7 days at an approximate split ratio of 1:3 to 1:5.

Single-cell hESC adaptation was performed according to protocols described previously (Ellerstrom et al., 2007; Hasegawa et al., 2006; Phillips et al., 2008a, 2008b). Briefly, hESC were dissociated using TrypLE (Invitrogen) for 5 min, gently triturated, diluted with 3 ml medium, passed through a cell strainer (70 μm), and plated at a density of 5.5×10^4 hESC/cm^2 on an Ortec feeder layer. The cells were split every 7 days with approximately 1/7 split ratios.

Preparation of hESC suspensions for transplantation

For routine inoculation of 3 mice, a 10-cm plate of undifferentiated hESC (typically yielding 3– 5×10^6 hESC) or an equal amount of differentiated hESC generated as described previously (Graichen et al., 2007; Phillips et al., 2007) was washed once with PBS and harvested with a cell scraper. The cell suspension was collected into a 15-ml falcon tube and spun down at 2000 rpm for 4 min. The cell pellet was carefully resuspended by stepwise addition of either room temperature PBS or a 1:1 mixture of PBS:Matrigel (BD Biosciences) to a final total volume of 150 μl (kept on ice), or mixed with 10^6 mitomycin C-treated CCD919 fibroblasts (viability >95%) that were previously shown to support hESC growth *in vitro*. Just prior to inoculation (<1 h after cell harvest), the cell suspension was equally divided into three tubes. Alternatively, individual hESC colonies (typically 30 000 hESC/colony as assessed by trypsin digest of individual colonies) were manually dislodged by cutting with a glass capillary tube, or single-cell suspensions of defined hESC numbers were generated. These samples were resuspended and prepared for injection as described above.

For beta cells or cardiomyocytes derived from long-term protocols using hES3 or GFP-hES3 cells (Phillips et al., 2007; Graichen et al., 2007), cell aggregates were physically disrupted by forcing a dilute cell suspension (content of a 10-cm plate in 5 ml) through a series of needles with progressively decreasing diameter (G21, G23, G25, G27). Digestions of parallel cell samples were performed using TrypLE (Invitrogen) for 5 min to estimate cell numbers.

hESC inoculation into various transplantation sites in mice

All studies were undertaken with prior approval from BRC (Biological Resource Center, Biopolis Singapore) Institutional Animal Care and Use Committee (IACUC No. 050008), and the National University of Singapore Institutional Review Board (NUS IRB No. 05-020). Male SCID mice (8–12 weeks age) were used for all experiments. All procedures were carried out in a biological safety cabinet under sterile conditions using sterile materials.

hESC suspensions (50 μl) were injected intramuscularly, subcutaneously, or intraperitoneally without anesthesia. For im injections, a sterile 1 ml syringe with a 23G needle was guided into the hind leg quadricep along its long axis and toward the muscle center. Injections of hESC into the kidney capsule, testis, epididymal fat pad, and liver were done under anesthesia. Mice received the following anesthetics and analgesics: Hypnorm (fentanyl/fluanisone, 0.2 ml/kg) or

ketamine (75 mg/kg ip)/Medetomidine (0.1 mg/kg ip), and a single dose of the antibiotic cephalexin 15 mg/kg (sc). Kidney capsule injections were carried out essentially as described (Nagy et al., 2003) with the following modifications: a 50-μl Hamilton syringe was attached to transparent, flexible HPLC grade tubing (inner diameter: 0.3 mm, length: 1.5 cm) that was used to deliver hESC suspensions into the renal subcapsular space. The tubing probed no further than 2 to 3 mm beyond the small opening in the kidney capsule before the cell material was discharged with gentle and constant pressure. The body wall was sutured with 3 stitches using absorbable suturing material, and the dermis with another 3–5 stitches using nonabsorbable suturing material.

For hESC injection into the testis, a 1-cm longitudinal incision in the abdominal wall was made, and the testis exteriorized. hESC were inoculated into the testis parenchyma with a modified Hamilton pipette, and the wound was sutured as described above. For hESC injection into the epididymal fat pad, a 1- to 2-cm ventral midline incision (first the epidermis, then the body wall) was made. The testis with the attached epididymal fat pad was exposed, and the hESC suspension injected into the center of the fat pad using a 23G needle, followed by suturing of the wound. For injection of hESC into the liver, a short dorsal midline incision was made just below the sternum (2–3 cm), (epidermis, then body wall). The large left liver lobe was exposed, and the hESC suspension slowly injected into the center of the large lobe using a 27G needle. Correct injection was visibly monitored by a rapid color change in the liver lobe (from red to light brown to red). After successful injection, the needle was retracted swiftly, the injection site was pressed with a cotton swab for about 1 min, and then a sterile, resorbable wound pad was placed at the injection site.

Quantification of teratoma formation

Teratomas developing in the testis, kidney capsule, liver, or epididymal fat pad are not readily visible, whereas those growing sc can be easily seen and measured using the traditional caliper method. For im inoculations, which were used most extensively in this study, teratoma formation was monitored visually using a simple grading system that was confirmed by caliper measurements: grade 0 = no teratoma visible (6.32-mm average maximal hind leg diameter, $n = 10$ for all groups); grade 1 = teratoma just detectable (10.55 mm average); grade 2 = teratoma obvious (13.2 mm average); and grade 3 = teratoma impedes locomotion (14.52 mm average). Grade 3 teratomas typically weigh 1–2 g and are harvested and processed for histology.

Tissue preparation, immunohistochemistry, and assessment of germ-layer distribution

After euthanasia of mice with rising CO_2 levels, teratomas were carefully excised from the surrounding muscle tissue, cut into 0.5-g pieces and fixed in Bouin's solution followed by paraffin sectioning. Five-micrometer sections were cut (Leica RM2255), and stored at 4 °C prior to staining or immunohistochemistry. All hematoxylin and eosin and immunostains were performed according to standard protocols. Teratomas were assessed by a board-certified pathologist at the Department of Pathology, National University of Singapore (T. Putti). As routinely performed in histology assessments of naturally occurring human teratomas, the composition of each teratoma was estimated semiquantitatively by visual inspection of H&E-stained sections in a blinded fashion. Differentiated elements in the teratomas were classified into ectodermal (skin, neural, etc.), endodermal (glandular structures), and mesodermal (cartilage, bone) components as a percentage of entire tissue. The remaining undifferentiated spindle stromal component was included under mesoderm.

Immunostaining was performed using the DAB detection system (Vectastain peroxidase, Vector Labs). Slides were counterstained with hematoxylin to identify nuclei. Primary antibodies used were anti-desmin (clone D39 from Dako, 1/50); anti-GFAP (mouse monoclonal clone 6F2 from Serotec, 1/50); anti-endoA cytokeratin (Troma-1 from Developmental Studies Hybridoma Bank, 1/20); and anti-Ki67 (MM1/Lki67 clone from Novocastra, 1/50).

Acknowledgments

We thank Alan Colman, Jeremy Crook, Ralph Graichen, Robert Zweigerdt, Sean Morrison, and Adrian Gee for helpful suggestions and comments on the manuscript. Declan Lunny is acknowledged for his crucial histology support.

Appendix A. Supplementary data

Supplementary data associated with this article can be found, in the online version, at doi:10.1016/j.scr.2009.02.002.

References

Adewumi, O., Aflatoonian, B., Ahrlund-Richter, L., Amit, M., Andrews, P.W., Beighton, G., Bello, P.A., Benvenisty, N., Berry, L.S., Bevan, S., et al., 2007. Characterization of human embryonic stem cell lines by the International Stem Cell Initiative. Nat. Biotechnol. 25, 803–816.

Amit, M., Margulets, V., Segev, H., Shariki, K., Laevsky, I., Coleman, R., Itskovitz-Eldor, J., 2003. Human feeder layers for human embryonic stem cells. Biol. Reprod. 68, 2150–2156.

Blum, B., Benvenisty, N., 2007. Clonal analysis of human embryonic stem cell differentiation into teratomas. Stem Cells 258, 1924–1930.

Blum, B., Benvenisty, N., 2008. The tumorigenicity of human embryonic stem cells. Adv. Cancer Res. 100, 133–158.

Bongso, A., Fong, C.Y., Ng, S.C., Ratnam, S., 1994. Human embryonic behavior in a sequential human oviduct-endometrial coculture system. Fertil. Steril. 61, 976–978.

Brederlau, A., Correia, A.S., Anisimov, S.V., Elmi, M., Roybon, L., Paul, G., Morizane, A., Bergquist, F., Riebe, I., Nannmark, U., et al., 2006. Transplantation of human embryonic stem cell-derived cells to a rat model of Parkinson's disease: effect of in vitro differentiation on graft survival and teratoma formation. Stem Cells 24, 1433–1440.

Brivanlou, A.H., Gage, F.H., Jaenisch, R., Jessell, T., Melton, D., Rossant, J., 2003. Setting standards for human embryonic stem cells. Science 300, 913–916.

Cai, J., Yi, F.F., Yang, X.C., Lin, G.S., Jiang, H., Wang, T., Xia, Z., 2007. Transplantation of embryonic stem cell-derived cardiomyocytes improves cardiac function in infarcted rat hearts. Cytotherapy 9, 283–291.

Choo, A.B., Padmanabhan, J., Chin, A.C., Oh, S.K., 2004. Expansion of pluripotent human embryonic stem cells on human feeders. Biotechnol. Bioeng. 88, 321–331.

Choo, A.B.H., Tan, H.L., Ang, S.N., Fong, W.J., Chin, A.C.P., Lo, J.C.Y., Zheng, L., Hentze, H., Philp, R.J., Oh, S.K.W., et al., 2008. Selection against undifferentiated human embryonic stem cells by a cytotoxic antibody recognizing podocalyxin-like protein-1. Stem Cells 26, 1454–1463.

Cooke, M.J., Stojkovic, M., Przyborski, S.A., 2006. Growth of teratomas derived from human pluripotent stem cells is influenced by the graft site. Stem Cells Dev. 15, 254–259.

Costa, M., Dottori, M., Ng, E., Hawes, S.M., Sourris, K., Jamshidi, P., Pera, M.F., Elefanty, A.G., Stanley, E.G., 2005. The hESC line Envy expresses high levels of GFP in all differentiated progeny. Nat. Methods 2, 259–260.

Crook, J., Peura, T.T., Kravets, L., Bosman, A.G., Buzzard, J.J., Horne, R., Hentze, H., Zweigerdt, R., Chua, F., Upshall, A., et al., 2007. The generation of six clinical-grade human embryonic stem cell lines. Cell Stem Cell 1, 490–494.

Damjanov, I., Andrews, P.W., 2007. The terminology of teratocarcinomas and teratomas. Nat. Biotechnol. 25, 1212.

De Coppi, P., Bartsch Jr., G., Siddiqui, M.M., Xu, T., Santos, C.C., Perin, L., Mostoslavsky, G., Serre, A.C., Snyder, E.Y., Yoo, J.J., et al., 2007. Isolation of amniotic stem cell lines with potential for therapy. Nat. Biotechnol. 25, 100–106.

Dressel, R., Schindehutte, J., Kuhlmann, T., Elsner, L., Novota, P., Baier, P.C., Schillert, A., Bickeboller, H., Herrmann, T., Trenkwalder, C., et al., 2008. The tumorigenicity of mouse embryonic stem cells and in vitro differentiated neuronal cells is controlled by the recipients' immune response. PLoS ONE 3, e2622.

Drukker, M., Katchman, H., Katz, G., Even-Tov Friedman, S., Shezen, E., Hornstein, E., Mandelboim, O., Reisner, Y., Benvenisty, N., 2006. Human embryonic stem cells and their differentiated derivatives are less susceptible to immune rejection than adult cells. Stem Cells 24, 221–229.

Eshpeter, A., Jiang, J., Au, M., Rajotte, R.V., Lu, K., Lebkowski, J.S., Majumdar, A.S., Korbutt, G.S., 2008. In vivo characterization of transplanted human embryonic stem cell-derived pancreatic endocrine islet cells. Cell Prolif. 41, 843–858.

Ellerstrom, C., Strehl, R., Noaksson, K., Hyllner, J., Semb, H., 2007. Facilitated expansion of human embryonic stem cells by single cell enzymatic dissociation. Stem Cells 25, 1690–1696.

FDA, 2006. Supplemental guidance on testing for replication competent retrovirus in retroviral vector based gene therapy products and during follow-up of patients in clinical trials using retroviral vectors. http://www.fda.gov/CBER/gdlns/retrogt1000.pdf.

FDA, 2008a. Cellular therapies derived from human embryonic stem cells—considerations for pre-clinical safety testing and patient monitoring. http://www.fda.gov/ohrms/dockets/ac/08/briefing/2008-0471B1_1.pdf.

FDA, 2008b. Cellular therapies derived from human embryonic stem cells scientific http://wwwfdagov/ohrms/dockets/ac/cber08html#CellularTissueGeneTherapies.

Fujikawa, T., Oh, S.H., Pi, L., Hatch, H.M., Shupe, T., Petersen, B.E., 2005. Teratoma formation leads to failure of treatment for type I diabetes using embryonic stem cell-derived insulin-producing cells. Am. J. Pathol. 166, 1781–1791.

Gertow, K., Cedervall, J., Unger, C., Szoke, K., Blennow, E., Imreh, M.P., Ahrlund-Richter, L., 2007. Trisomy 12 in HESC leads to no selective in vivo growth advantage in teratomas, but induces an increased abundance of renal development. J. Cell. Biochem. 100, 1518–1525.

Gertow, K., Wolbank, S., Rozell, B., Sugars, R., Andang, M., Parish, C.L., Imreh, M.P., Wendel, M., Ahrlund-Richter, L., 2004. Organized development from human embryonic stem cells after injection into immunodeficient mice. Stem Cells Dev. 13, 421–435.

Graichen, R., Xu, X., Braam, S.R., Balakrishnan, T., Norfiza, S., Sieh, S., Soo, S.Y., Tham, S.C., Mummery, C., Colman, A., et al., 2007. Enhanced cardiomyogenesis of human embryonic stem cells by a small molecular inhibitor of p38 MAPK. Differentiation 76, 357–370.

Guo, X.M., Zhao, Y.S., Chang, H.X., Wang, C.Y., E, L.L., Zhang, X.A., Duan, C.M., Dong, L.Z., Jiang, H., Li, J., et al., 2006. Creation of engineered cardiac tissue in vitro from mouse embryonic stem cells. Circulation 113, 2229–2237.

Halme, D.G., Kessler, D.A., 2006. FDA regulation of stem-cell-based therapies. N. Engl. J. Med. 355, 1730–1735.

Hasegawa, K., Fujioka, T., Nakamura, Y., Nakatsuji, N., Suemori, H., 2006. A method for the selection of human embryonic stem cell sublines with high replating efficiency after single-cell dissociation. Stem Cells 24, 2649–2660.

Hentze, H., Graichen, R., Colman, A., 2007. Cell therapy and the safety of embryonic stem cell-derived grafts. Trends Biotechnol. 25, 24–32.

Keller, G., 2005. Embryonic stem cell differentiation: emergence of a new era in biology and medicine. Genes Dev. 19, 1129–1155.

Kelly, P.N., Dakic, A., Adams, J.M., Nutt, S.L., Strasser, A., 2007. Tumor growth need not be driven by rare cancer stem cells. Science 317, 337.

Kroon, E., Martinson, L.A., Kadoya, K., Bang, A.G., Kelly, O.G., Eliazer, S., Young, H., Richardson, M., Smart, N.G., Cunningham, J., et al., 2008. Pancreatic endoderm derived from human embryonic stem cells generates glucose-responsive insulin-secreting cells in vivo. Nat. Biotechnol. 26, 443–452.

Kumashiro, Y., Asahina, K., Ozeki, R., Shimizu-Saito, K., Tanaka, Y., Kida, Y., Inoue, K., Kaneko, M., Sato, T., Teramoto, K., et al., 2005. Enrichment of hepatocytes differentiated from mouse embryonic stem cells as a transplantable source. Transplantation 79, 550–557.

Laflamme, M.A., Gold, J., Xu, C., Hassanipour, M., Rosler, E., Police, S., Muskheli, V., Murry, C.E., 2005. Formation of human myocardium in the rat heart from human embryonic stem cells. Am. J. Pathol. 167, 663–671.

Lawrenz, B., Schiller, H., Willbold, E., Ruediger, M., Muhs, A., Esser, S., 2004. Highly sensitive biosafety model for stem-cell-derived grafts. Cytotherapy 6, 212–222.

Leist, M., Bremer, S., Brundin, P., Hescheler, J., Kirkeby, A., Krause, K.H., Poerzgen, P., Puceat, M., Schmidt, M., Schrattenholz, A., et al., 2008. The biological and ethical basis of the use of human embryonic stem cells for in vitro test systems or cell therapy. ALTEX 25, 163–190.

Lensch, M.W., Ince, T.A., 2007. The terminology of teratocarcinomas and teratomas. Nat. Biotechnol. 25, 1211.

Nagy, A., Gertsentein, M., Vintersten, K., Behringer, R., 2003. Manipulating the Mouse Embryo. Cold Spring Harbor Laboratory Press, Cold Spring Harbor, NY.

Phillips, B., Hentze, H., Rust, W., Chen, Q., Chipperfield, H., Tan, E.K., Abraham, S., Sadasivam, A., Soong, P.L., Wang, S.T., et al., 2007. Directed differentiation of human embryonic stem cells into the pancreatic endocrine lineage. Stem Cells Dev. 16, 561–578.

Phillips, B.W., Lim, R.Y., Tan, T.T., Rust, W.L., Crook, J.M., 2008a. Efficient expansion of clinical-grade human fibroblasts on microcarriers: cells suitable for ex vivo expansion of clinical-grade hESCs. J. Biotechnol. 134, 79–87.

Phillips, B.W., Horne, R., Lay, T.S., Rust, W.L., Teck, T.T., Crook, J.M., 2008b. Attachment and growth of human embryonic stem cells on microcarriers. J. Biotechnol. 138, 24–32.

Plaia, T.W., Josephson, R., Liu, Y., Zeng, X., Ording, C., Toumadje, A., Brimble, S.N., Sherrer, E.S., Uhl, E.W., Freed, W.J., et al., 2006. Characterization of a new NIH-registered variant human embryonic stem cell line, BG01V: a tool for human embryonic stem cell research. Stem Cells 24, 531–546.

Prokhorova, T.A., Harkness, L.M., Frandsen, U., Ditzel, N., Burns, J.S., Schroeder, H.D., Kassem, M., 2008. Teratoma formation by

human embryonic stem cells is site-dependent and enhanced by the presence of matrigel. Stem Cells Dev., in press (doi:10.1089/scd.2007.0266).

Przyborski, S.A., 2005. Differentiation of human embryonic stem cells after transplantation in immune-deficient mice. Stem Cells 23, 1242–1250.

Quintana, E., Shackleton, M., Sabel, M.S., Fullen, D.R., Johnson, T.M., Morrison, S.J., 2008. Efficient tumour formation by single human melanoma cells. Nature 456, 593–598.

Reubinoff, B.E., Itsykson, P., Turetsky, T., Pera, M.F., Reinhartz, E., Itzik, A., Ben-Hur, T., 2001. Neural progenitors from human embryonic stem cells. Nat. Biotechnol. 19, 1134–1140.

Reubinoff, B.E., Pera, M.F., Fong, C.Y., Trounson, A., Bongso, A., 2000. Embryonic stem cell lines from human blastocysts: somatic differentiation in vitro. Nat. Biotechnol. 18, 399–404.

Shibata, H., Ageyama, N., Tanaka, Y., Kishi, Y., Sasaki, K., Nakamura, S., Muramatsu, S., Hayashi, S., Kitano, Y., Terao, K., et al., 2006. Improved safety of hematopoietic transplantation with monkey embryonic stem cells in the allogeneic setting. Stem Cells 24, 1450–1457.

Solter, D., 2006. From teratocarcinomas to embryonic stem cells and beyond: a history of embryonic stem cell research. Nat. Rev. Genet. 7, 319–327.

Stojkovic, P., Lako, M., Stewart, R., Przyborski, S., Armstrong, L., Evans, J., Murdoch, A., Strachan, T., Stojkovic, M., 2005. An autogeneic feeder cell system that efficiently supports growth of undifferentiated human embryonic stem cells. Stem Cells 23, 306–314.

Takahashi, K., Tanabe, K., Ohnuki, M., Narita, M., Ichisaka, T., Tomoda, K., Yamanaka, S., 2007. Induction of pluripotent stem cells from adult human fibroblasts by defined factors. Cell 131, 861–872.

Thomson, J.A., Itskovitz-Eldor, J., Shapiro, S.S., Waknitz, M.A., Swiergiel, J.J., Marshall, V.S., Jones, J.M., 1998. Embryonic stem cell lines derived from human blastocysts. Science 282, 1145–1147.

Tian, X., Woll, P.S., Morris, J.K., Linehan, J.L., Kaufman, D.S., 2006. Hematopoietic engraftment of human embryonic stem cell-derived cells is regulated by recipient innate immunity. Stem Cells 24, 1370–1380.

Tomescot, A., Leschik, J., Bellamy, V., Dubois, G., Messas, E., Bruneval, P., Desnos, M., Hagege, A.A., Amit, M., Itskovitz, J., et al., 2007. Differentiation in vivo of cardiac committed human embryonic stem cells in post-myocardial infarcted rats. Stem Cells 25, 2200–2205.

Tzukerman, M., Rosenberg, T., Reiter, I., Ben-Eliezer, S., Denkberg, G., Coleman, R., Reiter, Y., Skorecki, K., 2006. The influence of a human embryonic stem cell-derived microenvironment on targeting of human solid tumor xenografts. Cancer Res. 66, 3792–3801.

Vogel, G., 2005. Ready or not? Human ES cells head toward the clinic. Science 308, 1534–1538.

Xu, X.Q., Zweigerdt, R., Soo, S.Y., Ngoh, Z.X., Tham, S.C., Wang, S.T., Graichen, R., Davidson, B., Colman, A., Sun, W., 2008. Highly enriched cardiomyocytes from human embryonic stem cells. Cytotherapy 10, 376–389.

Yu, J., Vodyanik, M.A., Smuga-Otto, K., Antosiewicz-Bourget, J., Frane, J.L., Tian, S., Nie, J., Jonsdottir, G.A., Ruotti, V., Stewart, R., et al., 2007. Induced pluripotent stem cell lines derived from human somatic cells. Science 318, 1917–1920.

Zhang, S.C., Wernig, M., Duncan, I.D., Brustle, O., Thomson, J.A., 2001. In vitro differentiation of transplantable neural precursors from human embryonic stem cells. Nat. Biotechnol. 19, 1129–1133.